

Research Article

Backward Spectral Characterization of Liquid Crystal Display Based on Forward Spectral Characterization

Jian-qing Zhang,^{1,2} Fang Cai,² Xiao-ying Shen,³ Zhen Liu,¹ and Ming Zhu⁴

¹University of Shanghai for Science and Technology, Shanghai 200093, China

²College of Engineering, Qufu Normal University, Rizhao, Shandong 276826, China

³Navy Marine Environment Office, Beijing 100081, China

⁴Henan University of Engineering, Zhengzhou, Henan 451191, China

Correspondence should be addressed to Zhen Liu; lunaprint@163.com

Received 20 December 2015; Accepted 15 March 2016

Academic Editor: Michele Fedel

Copyright © 2016 Jian-qing Zhang et al. This is an open access article distributed under the Creative Commons Attribution License, which permits unrestricted use, distribution, and reproduction in any medium, provided the original work is properly cited.

A backward spectral characterization for Liquid Crystal Display by the use of rule for the maximum peak of spectral radiation curves changing with the digital input values is proposed; this new model is developed based on forward spectral characterization. It deals with estimation of *RGB* used as input to the digital display from known spectral radiation curves. We first investigate the rule for the peak of spectral radiation curves changing with the digital input values of primaries; then the initial digital input *RGB* are calculated based on that rule using the known spectral radiation curves ρ_0 . Third, *RGB* are inputted into forward spectral characterization model and the corresponding spectral radiation curves ρ_1 are predicted. Last, *RGB* are modified according to the difference between predicted ρ_1 and known ρ_0 , until this difference satisfied the prediction accuracy of the inverse characterization model. The inverse model has the advantage of using the same model for both forward and inverse color space transformation. This improves the accuracy of the color space transformation and reduces the source of errors. Results for 3 devices are shown and discussed; the accuracy of this model is considered sufficient for many applications.

1. Introduction

Liquid Crystal Display (LCD) has been widely used in the high accuracy requirement industrial practice field such as the color quality evaluation and screen soft proofing, owing to its high luminance, large contrast ratio, sharpness, spatial uniformity, and low power consumption. It is known that every color device has its characteristics, which makes color communication and reproduction difficult. To ensure color reproduction accuracy, color-characterization model needs to be applied to minimize the impact of device differences and preserve information during the communication of the color between devices.

Color-characterization model can be classified into two categories: colorimetric and spectral [1, 2]. The function of color-characterization is to define the relationship between device-dependent color spaces and device-independent color spaces; the typically device-dependent color spaces are *RGB*; typically device-independent color spaces are CIEXYZ or

CIELAB for colorimetric and spectral radiation curves for spectral characterization. The color characterization has two directions, that is, forward and backward transformation [3]; the former aims to predict CIEXYZ or CIELAB (for the colorimetric color-characterization model) or spectral radiation curves (for the spectral color-characterization model) for any set of digital input values [1, 2, 4–11], whereas the latter aims to generate right colors by providing a set of digital values of the input device [12–15].

Many forward and backward colorimetric color-characterization models for display device were proposed [4–7, 12, 13]. Although those models work well, they are constrained to a specific illuminant and observer due to metamerism. The model would be reestablished if illuminant or observer changes. The spectral radiation values are defined as an object “fingerprinting” that accurately represents important information of its color and composition, so spectral color reproduction could match originals under arbitrary illuminants and observers [14–16]. In the quest for more accurate color

reproduction, some spectral color-characterization models for color devices have been proposed in the literature [1, 8–11, 14, 15].

For LCD, Liu et al. [8–10] proposed some forward spectral color-characterization models; spectral radiation curves of any digital input triplet (d_r, d_g, d_b) values can be accurately predicted by those models. But how can we display a desired color with known spectral radiation curves? So far there has been little work done for the backward spectral color-characterization model. This makes spectral color reproduction difficulty on the display device. This paper focuses on the backward spectral model which is to estimate the digital input values input to the device in order to display the desired color sensation.

This paper proposes a novel backward spectral color-characterization model based on forward model, according to the rule for the peak of spectral radiation curves changing with the digital input values. Using this model, the backward and forward color space transformation can be carried out only by utilizing the forward spectral color-characterization model. And this backward model does not require more measurements than those needed for setting up the forward model.

This paper is organized as follows. Section 2 describes the theory of the backward spectral color-characterization model based on forward model. Section 3 presents experimental results and evaluation of the performance of the proposed method. Lastly, concluding remarks are provided in Section 4.

2. The Backward Spectral Color-Characterization Model Based on Forward Model

The backward spectral color-characterization model can be established based on any forward spectral color-characterization model. In this study, the SRPPM model was selected [10]. The backward model has two key steps: calculating the initial (d_r, d_g, d_b) values according to the rule for the peak of spectral radiation curves changing with the digital input values and adjusting the values of (d_r, d_g, d_b) to meet the accuracy requirement of the backward model.

2.1. The Spectral Radiance Piecewise Partition Model [8–10]. The interaction between channels was weak and spectral additivity property was held well, and the relations between spectral radiation values and digital input values at different wavelengths varied; that is, they were the functions of wavelength. According to the abovementioned, the calculation method based on piecewise spectral model was proposed, in which the relation between spectral radiation values and digital values was fitted by a cubic polynomial in each piece of wavelength with measured spectral radiation curves. The spectral radiation curves of *RGB* primaries with any digital values can be found out with measurements and fitted cubic polynomial in this way and then any displayed color can be turned out by the spectral additivity property of primaries at given digital input values [8, 9]. However, this model

was not well implemented when the digital input value was small; to overcome this problem, Tian et al. proposed the spectral radiance piecewise partition model (SRPPM) [10].

2.2. The Rule for the Peak of Spectral Radiation Curves Changing with the Digital Input Values. To determine the relationship between the digital input (d_r, d_g, d_b) values and the corresponding spectral radiation curves, we select 3 display devices in this study. All of the displays are three primaries *RGB* devices; they are EIZO CG246 (EIZO), NEC EA191M (NEC), and HP Compad LE1901W1 (HP). The colors displayed on those screens were measured. By analyzing the relationship between the digital input (d_r, d_g, d_b) values and the corresponding spectral radiation curves, the rules were found as follows (taking EIZO display as an example, as shown in Figure 1).

(1) For tertiary color, the spectral radiation curves change with the digital input (d_r, d_g, d_b) values; the rules were found as follows: there was very significant positive correlation between the spectral radiation values of wavelength in the rang 590 nm~780 nm and the value of d_r ; if the value of d_r changes, the spectral radiation value of this wavelength range changes very obviously, but the spectral radiation values of another wavelength range remained nearly unchanged, as shown in Figure 1(a); the curve in black color is the spectral radial curve with digital input values (192, 192, 192); the curve in red color is the spectral radial curve with digital input values (255, 192, 192); the main difference between these two curves is the spectral radiation values of wavelength in the rang 590 nm~780 nm. The situation of d_g and d_b is similar to that of d_r . Namely, the spectral radiation values of wavelength in the rang 490 nm~580 nm are of positive relevance with d_g ; the spectral radiation values of wavelength in the rang 430 nm~480 nm are of positive relevance with d_b , as shown in Figures 1(b) and 1(c).

The situation of the secondary color is similar to the situation of tertiary colors mentioned above.

(2) For red primary, the spectral radiation value of 650 nm is the largest; for green primary, the spectral radiation value of 520 nm is the largest; and for blue primary, the spectral radiation value of 450 nm is the largest, as shown in Figure 1(d).

The spectral radiation values of 650 nm, 520 nm, and 450 nm are defined as $R(650)$, $R(520)$, and $R(450)$, respectively. For all color samples, it can be found out that $R(650)$ has been influenced mainly by d_r and has rarely been influenced by d_g and d_b ; $R(520)$ has been influenced mainly by d_g and has rarely been influenced by d_r and d_b ; and $R(450)$ has been influenced mainly by d_b and has rarely been influenced by d_r and d_g . This law was named “rule for the peak of spectral radiation curves changing with the digital input values.” Function relations between spectral radiation values which are $R(650)$, $R(520)$, and $R(450)$ and their corresponding digital input values were imitated for primaries, as shown in (1). Those formulas are used to reversely solve the digital input values

$$R(650) = F1(d_r),$$

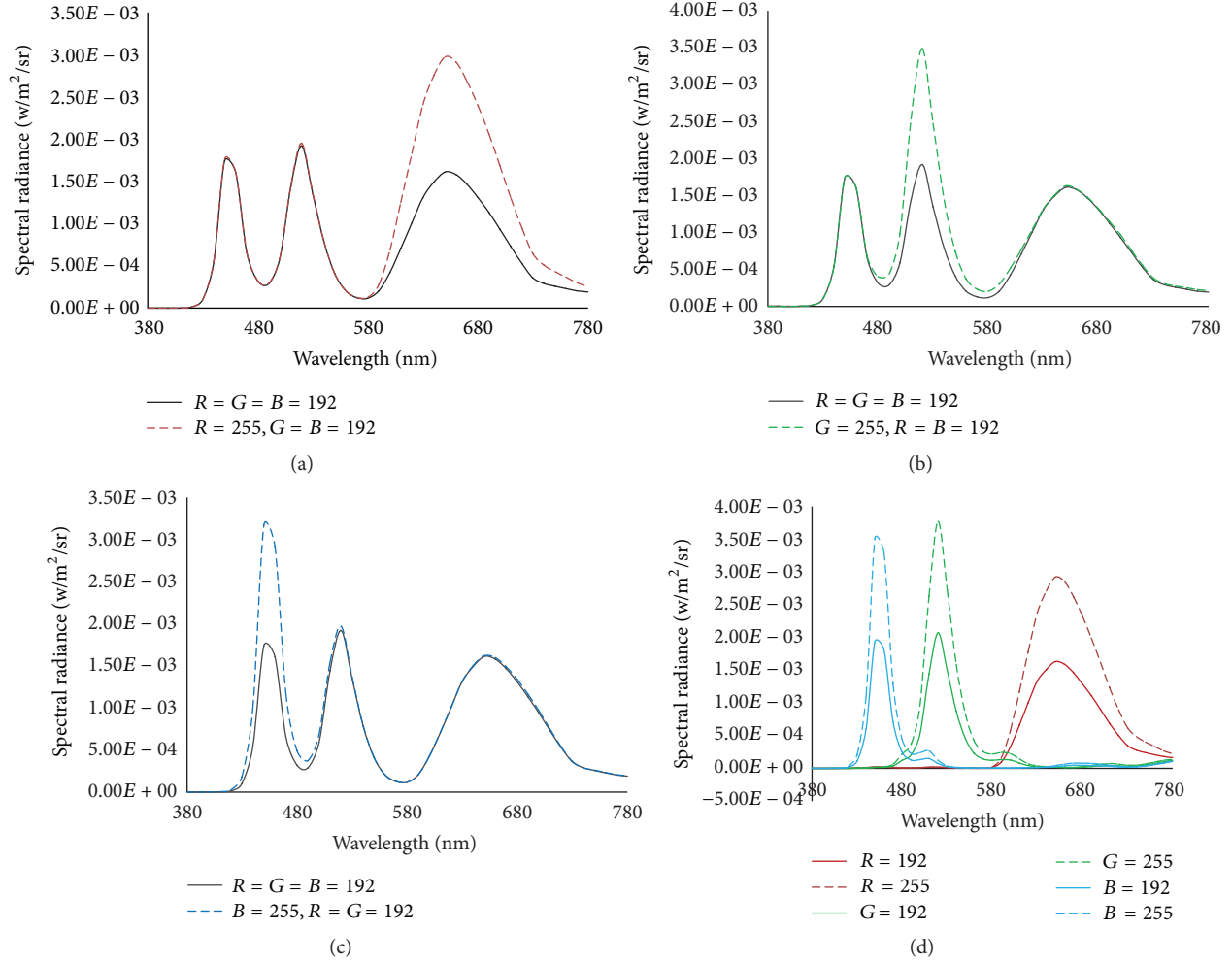


FIGURE 1: The spectral radiation curves with different digital input values for EIZO CG246.

$$\begin{aligned}
 R(520) &= F2(d_g), \\
 R(450) &= F3(d_b).
 \end{aligned}
 \tag{1}$$

HP and NEC also follow this rule; just spectrum peak values and stations of spectrum peak are different, and the function relations between spectrum peak values and their corresponding digital input values are different. For HP, the stations of spectrum peak of red, green, and blue are 610 nm, 530 nm, and 450 nm, respectively, for NEC, 610 nm, 550 nm, and 450 nm, respectively.

2.3. The Procedure for Calculating and Adjusting Initial (d_r, d_g, d_b) Values. Taking EIZO CG246 as an example, the procedure for calculating and adjusting initial (d_r, d_g, d_b) values is explained. The known spectral radiation curve is defined as ρ_0 and the spectral radiation values of the wavelength 650 nm, 520 nm, and 450 nm in ρ_0 are defined as $R_{\rho_0}(650)$, $R_{\rho_0}(520)$, and $R_{\rho_0}(450)$. The value of d_r is calculated using formula $F1$ shown in (1) and $R_{\rho_0}(650)$. d_g and d_b are calculated using $R_{\rho_0}(520)$ and $R_{\rho_0}(450)$ in a similar way, respectively.

Then (d_r, d_g, d_b) values are input to the forward model and the corresponding spectral curve of radial brightness ρ_1 is obtained; the difference between ρ_0 and ρ_1 is calculated and the color difference metric ΔE_{ab}^* and the spectrum mean square root deviation (SMSRD) are used to judge the prediction accuracy of model. $d_r, d_g,$ and d_b are considered as the predicted value of the inverse color-characterization model if ρ_1 satisfy the requirement of backward color-characterization precision. Otherwise, (d_r, d_g, d_b) should be modified, until ρ_1 satisfy the requirement of backward characteristic precision. The prediction precision requirement is $CD \leq 0.43\Delta E_{ab}^*$ (0.43 is 95ptl CD of forward model prediction error shown in Table 1) or $SMSRD \leq 0.08$ (0.08 is 95ptl SMSRD value of forward model prediction error shown in Table 1). When the calculated value does not meet the above conditions, the 300th cycle calculated data was chosen.

The spectral radiation values of the wavelength, 650 nm, 520 nm, and 450 nm, in ρ_1 are defined as $R_{\rho_1}(650)$, $R_{\rho_1}(520)$, and $R_{\rho_1}(450)$.

Figure 2 shows the flowchart of adjusting (d_r, d_g, d_b) values. First, the values of (d_r, d_g, d_b) are input into the forward color-characterization model and the spectral

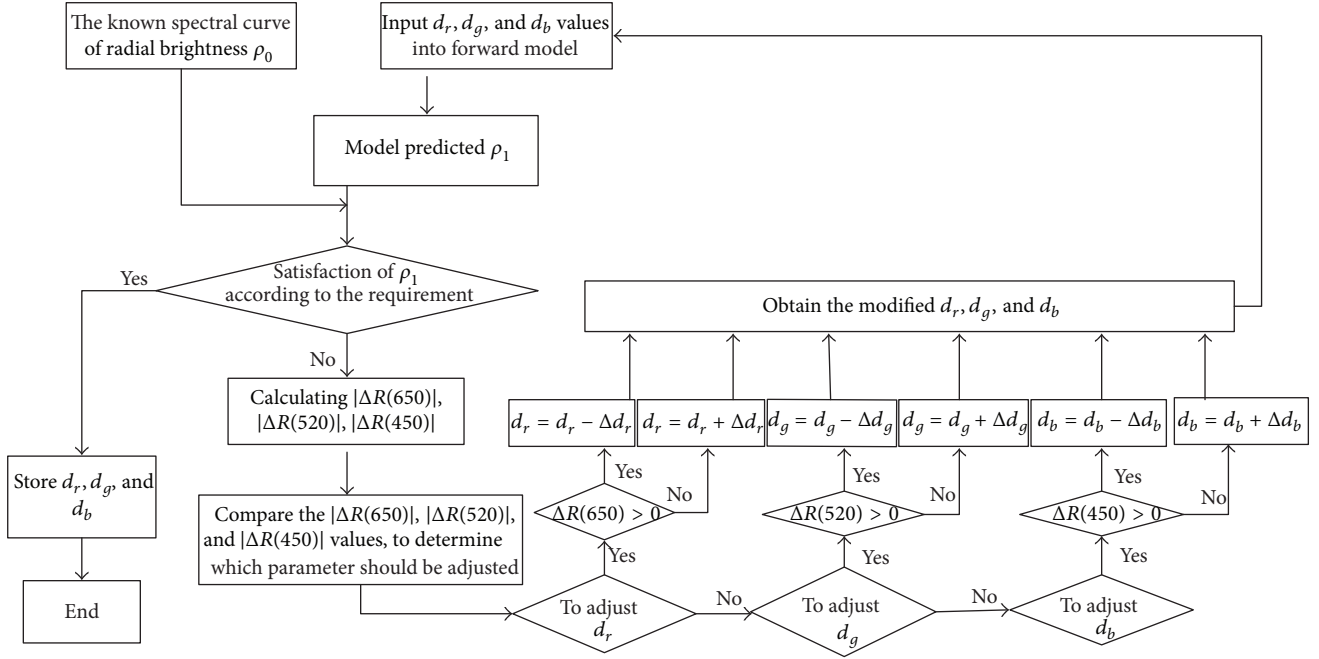


FIGURE 2: The modifying flow of digital input values d_r , d_g , and d_b .

TABLE 1: Difference between ρ_0 and ρ_1 of 216 test samples for forward color-characterization model.

Device	Items	Max.	Min.	Ave.	95ptl
EIZO	CD (ΔE_{ab}^*)	0.76	0	0.21	0.43
	SMSRD (%)	28.1	0	8.12	16.9
NEC	CD (ΔE_{ab}^*)	3.71	0.02	1.32	3.18
	SMSRD (%)	45.76	0.07	4.97	17.78
HP	CD (ΔE_{ab}^*)	5.9	0.38	1.64	3.13
	SMSRD (%)	10.07	0.1	2.96	6.6

radiation curves ρ_1 are thereby obtained. The values of $\Delta R(650)$, $\Delta R(520)$, and $\Delta R(450)$ are then calculated using

$$\begin{aligned}\Delta R(650) &= (R_{\rho_1}(650) - R_{\rho_0}(650)), \\ \Delta R(520) &= (R_{\rho_1}(520) - R_{\rho_0}(520)), \\ \Delta R(450) &= (R_{\rho_1}(450) - R_{\rho_0}(450)).\end{aligned}\quad (2)$$

Then the values of $|\Delta R(650)|$, $|\Delta R(520)|$, and $|\Delta R(450)|$ are compared to determine which parameter should be adjusted as follows.

d_r is modified if $|\Delta R(650)| \geq |\Delta R(520)|$ and $|\Delta R(650)| \geq |\Delta R(450)|$;

The output is new d_r and the old value d_r should be replaced. If $\Delta R(650) > 0$, $d_r = d_r - \Delta d_r$; else $d_r = d_r + \Delta d_r$;

d_g is modified if $|\Delta R(520)| \geq |\Delta R(450)|$ and $|\Delta R(520)| > |\Delta R(650)|$;

d_b is modified if $|\Delta R(450)| \geq |\Delta R(650)|$ and $|\Delta R(450)| \geq |\Delta R(520)|$;

d_r , d_g , and d_b are modified following the same approach shown in Figure 3; in this paper, $\Delta d_r = \Delta d_g = \Delta d_b = 1$.

Once the forward color-characterization model is selected, the calculation of ρ_1 is just a mathematical process. If the values of Δd_r , Δd_g , and Δd_b are smaller, the calculation of d_r , d_g , and d_b would be more accurate. Therefore, the precision of the backward color-characterization is mainly dominated by the forward model.

2.4. The Process Flow of Backward Color-Characterization Model. Figure 3 shows the flowchart of the backward characterization model. $R_{\rho_0}(650)$, $R_{\rho_0}(520)$, and $R_{\rho_0}(450)$ are inputs to the backward characterization model, and the corresponding (d_r, d_g, d_b) values are calculated by formulas shown in (1). Thereafter, the triplet (d_r, d_g, d_b) values are input into the forward spectral color-characterization model and the predicted spectral radiation curves ρ_1 can be obtained. The triplet (d_r, d_g, d_b) values are determined as the predictive values of the backward spectrum color-characterization model, while ρ_1 satisfy the accuracy of the backward model. Otherwise, the triplet (d_r, d_g, d_b) values will be modified until ρ_1 satisfy the model accuracy demand.

3. Experiment and Result

3.1. Apparatus. The instruments for measurements in this study are listed as follows: Konica-minolta CS-2000 Spectroradiometer (0.1/50 cm distance, aperture of 0.1°); displays

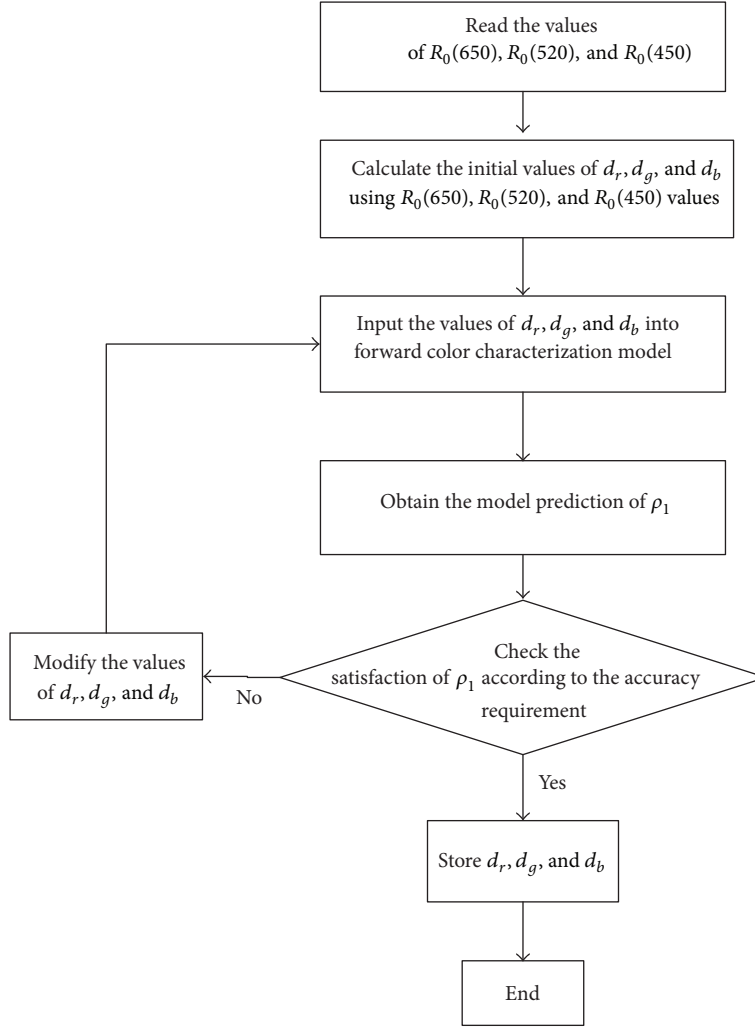


FIGURE 3: Flowchart of backward color-characteristic model based on forward model.

(calibration condition: D65 illumination, preheated for 1 h): EIZO CG 246 (EIZO), NEC EA191M (NEC), and HP Compad LE1901W1 (HP).

3.2. Sampling. Two datasets of RGB values were obtained in the experiment. The first dataset was three 16-step ramps from 0 to 255 for the red, green, and blue channels, respectively. These values were used to fit forward color-characterization models and function relations shown in (1). The second dataset was a verification set that consists of 216-color data with digital input, d_r , d_g and d_b , and the values were 0, 50, 100, 150, 200, and 255, respectively. They were used to verify the prediction precision of the forward and backward color-characterization models.

Measurements were taking place in dark room. A Spectroradiometer was placed at a distance of about 40 cm from the screen, perpendicularly to the screen surface.

All the spectral data used to calculate for models are 10 nm sampling interval.

3.3. Precision of the Forward Model and Backward Models

3.3.1. Precision of the Forward Model. To analyze the precision of models, the color difference metric ΔE_{ab}^* and the spectrum mean square root deviation (SMSRD) are applied. Precision of the forward model has a great influence on the accuracy of the backward model, so we firstly analyze the prediction accuracy of the forward models. The measured spectral radiation curves and the predicted spectral radiation curves by the forward model for triplet (d_r, d_g, d_b) are defined as ρ_0 and ρ_1 , respectively. The CD and SMSRD between ρ_0 and ρ_1 of 216 test samples are shown in Table 1. Here, we list the maximum, minimum, average, and 95th percentile (it is the value below which 95% of errors fall) of CD and SMSRD between ρ_0 and ρ_1 for the three devices. It is shown that SRPPM performed well; the average CD of the three devices are lower than $2\Delta E_{ab}^*$ units, which is considered to be sufficient for many applications, such as spectral image accurate representation, color quality evaluation, and screen soft proofing.

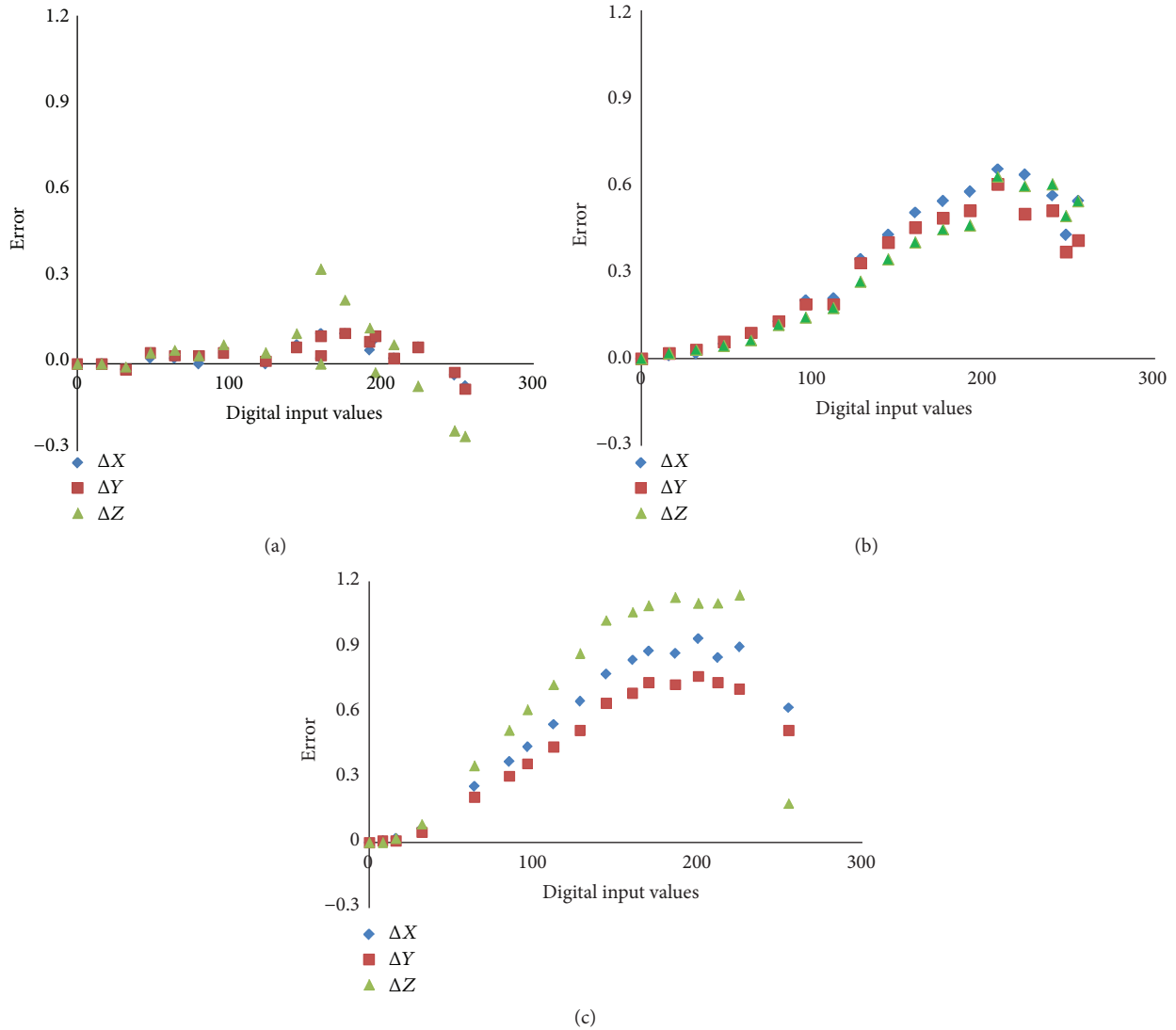


FIGURE 4: Channel dependence errors of different devices: (a) EIZO; (b) NEC; (c) HP.

The data in Table 1 show that there are no relevant relations between the SMSRD and CD; taking EIZO as an example, its average SMSRD value is the biggest, but its average CD is the smallest of the three devices. Therefore, SMSRD describes only the calculation accuracy for spectral radiation curves and cannot reflect color difference perceived by human eyes.

But the data in Table 1 show that the prediction accuracy of SRPPM model is different for different display. The prediction for EIZO is good; the average CD is $0.21\Delta E_{ab}^*$ and for the other two it is bad; the average CD is 1.32 and $1.64\Delta E_{ab}^*$, respectively. This is because the SRPPM model is built based on the assumption of channel independence. For displays with worse channel independence, the prediction of SRPPM model is worse. EIZO is a senior professional display device, NEC is a professional display device, and HP is a traditional display device; their channel dependence errors are different. Figure 4 demonstrates the channel dependence errors of three devices, where channel dependence errors are

equal to the measured relative tristimulus XYZ values of gray ($d_r = d_g = d_b$) minus the calculated relative tristimulus XYZ values of gray, under the assumption of channel independence. As shown in Figure 4, the channel independent error of EIZO is the smallest and of HP is the biggest. Therefore, the prediction precision of SRPPM model for EIZO is best among three devices.

3.3.2. Precision of the Backward Model. Using the backward color-characterization model, we can predict $(d_r, d_g, d_b)_{\text{pred}}$ for each of spectral radiation curves ρ_0 and can also predict the spectral radiation curves ρ_1 of each $(d_r, d_g, d_b)_{\text{pred}}$ with the forward color-characterization model. A four-triplet list is in the following form [12]:

$$\left\{ (d_r, d_g, d_b)_{\text{in}} \longrightarrow \rho_0 \longrightarrow (d_r, d_g, d_b)_{\text{pred}} \longrightarrow \rho_1 \right\}. \quad (3)$$

We computed RGB_{error} between the digital input $(d_r, d_g, d_b)_{\text{in}}$ and the model prediction $(d_r, d_g, d_b)_{\text{pred}}$ as well

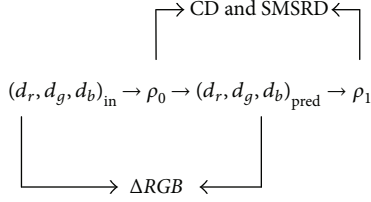


FIGURE 5: Computing errors.

TABLE 2: The difference between the measured values and predicted values of the inverse model.

Device	Items	Max.	Min.	Ave.	95ptl
EIZO	ΔRGB	19.00	0	4.98	14.00
	ΔR	19.00	-6.00	1.66	13.00
	ΔG	16.00	-1.00	1.94	12.00
	ΔB	13.00	-1.00	1.08	11.00
	CD (ΔE_{ab}^*)	2.97	0	0.36	0.80
	SMSRD (%)	27.01	0	8.10	17.12
NEC	ΔRGB	41.30	1.00	10.42	30.60
	ΔR	41.00	-3.00	7.23	30.00
	ΔG	22.00	-8.00	2.11	11.00
	ΔB	19.00	-8.00	2.79	11.00
	CD (ΔE_{ab}^*)	8.85	0.45	1.79	4.70
	SMSRD (%)	47.4	0.20	5.43	16.25
HP	ΔRGB	36.00	0	6.31	24.00
	ΔR	36.00	-14.00	1.07	24.00
	ΔG	25.00	-6.00	1.02	18.00
	ΔB	0	-10.00	1.72	0
	CD (ΔE_{ab}^*)	11.85	0.81	2.67	5.59
	SMSRD (%)	11.60	0.30	3.40	7.40

as spectral error between ρ_0 and ρ_1 , as shown in Figure 5 [12].

The values ΔRGB are calculated using

$$\Delta RGB = \sqrt{\Delta R^2 + \Delta G^2 + \Delta B^2}, \quad (4)$$

where ΔRGB is the total error of predicted values in the device-dependent RGB color spaces, ΔR is the error of red channel, ΔG and ΔB are the error for green and blue channel, respectively, and $\Delta R = (d_r)_{pred} - (d_r)_{in}$, $\Delta G = (d_g)_{pred} - (d_g)_{in}$, and $\Delta B = (d_b)_{pred} - (d_b)_{in}$.

In the quantitative evaluation of the backward models, CD, ΔRGB , ΔR , ΔG , ΔB , and SMSRD are applied, and the statistics of those items are provided in Table 2. The distribution of CD and ΔRGB is shown in Figures 6(a) and 6(b), respectively. It illustrated that the backward spectral color-characterization model is well implemented and the model prediction accuracy can satisfy the demand of different levels displays.

According to the statistics of CD shown in Table 2 and the histogram of CD distribution shown in Figure 6(a), the CD between measured ρ_0 and predicted ρ_1 of most samples are

smaller for three display devices; the average CD are $0.36\Delta E_{ab}^*$ unit for EIZO display, $1.79\Delta E_{ab}^*$ unit for NEC display, and $2.67\Delta E_{ab}^*$ unit for HP; and all of the CD are less than $3\Delta E_{ab}^*$ for EIZO display; 87.5% and 88.4% of the CD are less than $3\Delta E_{ab}^*$ for NEC and HP, respectively. For NEC and HP displays, there have a small amount of the CD are greater. Data of all samples in the experiment were analyzed and the result illustrated that large errors are localized at the dark color, whether for forward or for backward model. So the large prediction errors of backward model are mainly due to prediction error of forward model; additionally, because the spectral color space is not uniform, smaller error in spectral radiation curves between measured ρ_0 and predicted ρ_1 may produce large color difference while spectral radiation values are small.

According to the RGB difference (ΔRGB) shown in Table 2 and the histogram of RGB difference distribution shown in Figure 6(b), ΔRGB between known $(d_r, d_g, d_b)_{in}$ and predicted $(d_r, d_g, d_b)_{pred}$ of most samples are smaller for three display devices; the average ΔRGB are 4.98 for EIZO display, 10.42 for NEC display, and 6.31 for HP; and all of ΔRGB are less than 20 for EIZO display; 85.6% and 92.6% of the ΔRGB are less than 20 for NEC and HP, respectively. For NEC and HP displays, a small amount of ΔRGB between known $(d_r, d_g, d_b)_{in}$ and predicted $(d_r, d_g, d_b)_{pred}$ is great.

Model prediction accuracy for the blue channel is the best and for red channel it is the worst. We analyzed the triplet $(d_r, d_g, d_b)_{in}$ values and their corresponding predicted $(d_r, d_g, d_b)_{pred}$ values of all sample colors. The result shows that the error for tertiary color is almost zero; great errors are localized at secondary color and primary. When one value in the triplet $(d_r, d_g, d_b)_{in}$ of secondary color and primary equals 0, its corresponding predicted value has a larger error; meanwhile, the predicted value for other nonzero data has a small error.

4. Conclusion

While both forward (RGB to spectrum) and backward (spectrum to RGB) transforms are of interest to characterize a display, the backward transform is of higher importance as we pursue accurately specific colors on the considered display. This paper presents a backward spectral color-characterization model based on forward color-characterization model for LCD displays. The backward and forward characteristic can use single model, which improves the accuracy of color space transformation and reduces the source of the errors. The errors are found attributed mostly to the prediction precision of the forward model. This backward model does not require more measurements than those needed for setting up the forward model. This feature is beneficial to real-time calculation of the forward and backward color space conversion for a normal LCD display.

Competing Interests

The authors declare that they have no competing interests.

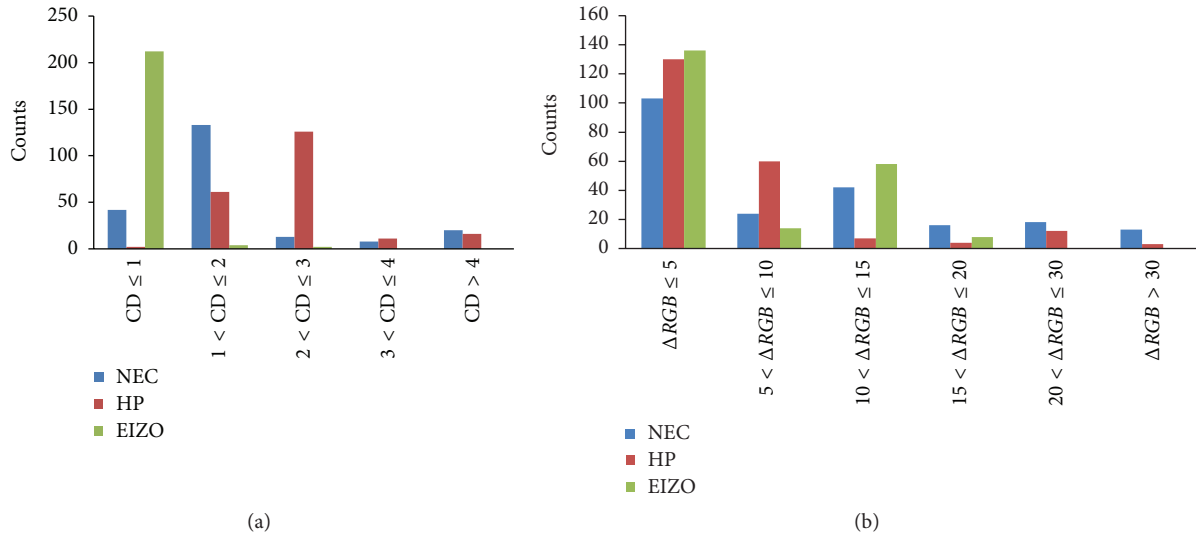


FIGURE 6: (a) Histogram of the color difference distribution of backward model and (b) histogram of ΔRGB distribution of backward model.

Acknowledgments

This study was supported by the National Natural Science Foundation of China (no. 61301231) and the Innovation Fund Project for Graduate Student of Shanghai (no. JWCXSL1201).

References

- [1] H.-L. Shen and J. H. Xin, "Spectral characterization of a color scanner by adaptive estimation," *Journal of the Optical Society of America A*, vol. 21, no. 7, pp. 1125–1130, 2004.
- [2] H.-L. Shen and J. H. Xin, "Colorimetric and spectral characterization of a color scanner using local statistics," *Journal of Imaging Science and Technology*, vol. 48, no. 4, pp. 342–346, 2004.
- [3] J. B. Thomas, P. Colantoni, J. Y. Hardeberg et al., *Advanced Color Image Processing and Analysis*, Springer Science, Business Media, New York, NY, USA, 2013.
- [4] Y. S. Kwak and W. M. Lindsay, "Accurate prediction of colors on liquid crystal displays," in *Proceedings of the IS&T/SID 9th Color Imaging Conference*, 11 pages, Scottsdale, Ariz, USA, November 2001.
- [5] S. Wen and R. Wu, "Two-primary crosstalk model for characterizing liquid crystal displays," *Color Research and Application*, vol. 31, no. 2, pp. 102–108, 2006.
- [6] R. Safaee-Rad and M. Aleksic, "R/G/B color crosstalk characterization and calibration for LCD displays," in *Color Imaging XVI: Displaying, Processing, Hardcopy, and Applications*, vol. 7866 of *Proceedings of SPIE*, pp. 1–12, San Francisco, Calif, USA, January 2011.
- [7] J.-B. Thomas, J. Y. Hardeberg, I. Foucherot, and P. Gouton, "The PLVC display color characterization model revisited," *Color Research and Application*, vol. 33, no. 6, pp. 449–460, 2008.
- [8] H.-X. Liu, L. Zheng, L. Dai, M. Huang, and B. Wu, "Color characterization of LCD based on spectral additive properties," *Acta Optica Sinica*, vol. 31, no. 12, Article ID 1233002, 2011.
- [9] H.-X. Liu, G.-H. Cui, M. Huang, B. Wu, Y.-F. Xu, and M. Luo, "Colorimetric characterization of LCD based on wavelength partition spectral model," *Spectroscopy and Spectral Analysis*, vol. 33, no. 10, pp. 2751–2757, 2013.
- [10] Q.-H. Tian, Z. Liu, H.-Q. Yu, D.-M. Zhao, and S.-W. Liu, "The spectral radiance piecewise partition model for characterizing liquid crystal displays," *Displays*, vol. 39, pp. 133–138, 2015.
- [11] R. Balasubramanian, "The use of spectral regression in modeling halftone color printers," in *Proceedings of the IS&T/OSA Annual Conference, Optics & Imaging in the Information Age*, pp. 372–375, Rochester, NY, USA, 1996.
- [12] L. Blondé, J. Stauder, and B. Lee, "Inverse display characterization: a two-step parametric model for digital displays," *Journal of the Society for Information Display*, vol. 17, no. 1, pp. 13–21, 2009.
- [13] J.-B. Thomas, P. Colantoni, J. Y. Hardeberg, I. Foucherot, and P. Gouton, "A geometrical approach for inverting display color-characterization models," *Journal of the Society for Information Display*, vol. 16, no. 10, pp. 1021–1031, 2008.
- [14] B. Sun, H. Liu, and S. Zhou, "Spectral separation for multi-spectral image reproduction based on constrained optimization method," *Journal of Spectroscopy*, vol. 2014, Article ID 345193, 8 pages, 2014.
- [15] P. Urban and R.-R. Grigat, "Spectral-based color separation using linear regression iteration," *Color Research and Application*, vol. 31, no. 3, pp. 229–238, 2006.
- [16] H.-L. Shen and J. H. Xin, "Estimation of spectral reflectance of object surfaces with the consideration of perceptual color space," *Optics Letters*, vol. 32, no. 1, pp. 96–98, 2007.

